Journal of Physiology (2002), **541.1**, *pp.* 159–167
DOI: 10.1113/jphysiol.2001.013268

www.jphysiol.org

Facilitation of intracellular H^+ ion mobility by CO_2/HCO_3^- in rabbit ventricular myocytes is regulated by carbonic anhydrase

K. W. Spitzer *, R. L. Skolnick *, B. E. Peercy †, J. P. Keener † and R. D. Vaughan-Jones ‡

* *Nora Eccles Harrison Cardiovascular Research and Training Institute and † Department of Mathematics, University of Utah, Salt Lake City, UT, USA and ‡ University Laboratory of Physiology, Parks Road, Oxford OX1 3PT, UK*

Intracellular H^+ mobility was estimated in the rabbit isolated ventricular myocyte by diffusing HCl into the cell from a patch pipette, while imaging pH_i confocally using intracellular ratiometric SNARF fluorescence. The delay for acid diffusion between two downstream regions ~40 μm apart was reduced from ~25 s to ~6 s by replacing Hepes buffer in the extracellular superfusate with a 5 % CO_2/HCO_3^- buffer system (at constant pH_o of 7.40). Thus CO_2/HCO_3^- (carbonic) buffer facilitates apparent H_i^+ mobility. The delay with carbonic buffer was increased again by adding acetazolamide (ATZ), a membrane permeant carbonic anhydrase (CA) inhibitor. Thus facilitation of apparent H_i^+ mobility by CO_2/HCO_3^- relies on the activity of intracellular CA. By using a mathematical model of diffusion, the apparent intracellular H^+ equivalent diffusion coefficient (D_{app}^H) in CO_2/HCO_3^--buffered conditions was estimated to be 21.9×10^{-7} cm^2 s^{-1}, 5.8 times faster than in the absence of carbonic buffer. Facilitation of H_i^+ mobility is discussed in terms of an intracellular carbonic buffer shuttle, catalysed by intracellular CA. Turnover of this shuttle is postulated to be faster than that of the intrinsic buffer shuttle. By regulating the carbonic shuttle, CA regulates effective H_i^+ mobility which, in turn, regulates the spatiotemporal uniformity of pH_i. This is postulated to be a major function of CA in heart.

(Received 10 September 2001; accepted after revision 8 February 2002)
Corresponding author K. W. Spitzer: Nora Eccles Harrison Cardiovascular Research and Training Institute, University of Utah, Salt Lake City, UT, USA. Email: spitzer@cvrti.utah.edu

The accompanying paper (Vaughan-Jones *et al.* 2002) reported that, in rabbit ventricular myocytes, the apparent diffusion coefficient for the intracellular H^+ ion (D_{app}^H) or its ionic equivalent such as OH^- is ~300-fold lower than in dilute, unbuffered solution, and about 55-fold lower than that for simple inorganic ions like Na^+ or K^+. This value of D_{app}^H represents the intrinsic mobility of H^+ equivalents in the cytoplasmic compartment, determined *in situ* in the absence of an intracellular CO_2/HCO_3^- buffer system. The consequence of a low D_{app}^H is that a spatially localized intracellular acidosis spreads slowly as a diffusive wave, taking more than 1 min to pass down the length of a 100 μm cardiac myocyte. Such slow kinetics of acid movement mean that acid/base transport at the sarcolemma may be expected to result in a spatial non-uniformity of pH_i, with unpredictable consequences for cardiac function.

The movement of cytoplasmic acid is likely to be limited by the mobility of intracellular buffers, as these bind almost all intracellular acid (Junge & McLaughlin, 1987; Irving *et al.* 1990). In cardiomyocytes, intrinsic H_i^+ mobility will therefore be defined by intracellular mobile buffers such as small peptides containing histidine (e.g. derivatives of carnosine, anserine and homocarnosine) and by intracellular taurine and P_i (see Table 1 of Vaughan-Jones *et al.* 2002). If this model of H_i^+ equivalent mobility is correct, adding a more mobile buffer to the intracellular compartment should increase intrinsic H_i^+ mobility.

CO_2/HCO_3^- is a physiological buffer system that would be expected to have relatively high effective mobility, as both CO_2 and HCO_3^- are low molecular weight solutes that lack specific intracellular binding proteins, at least in the heart, and which are non-charged or have low electronic valency. The ability of this buffer system to facilitate H_i^+ mobility may, however, be limited by the speed of the chemical interconversion of CO_2 and HCO_3^-, as the uncatalysed hydration of CO_2 is known to be slow (Swenson & Maren, 1978), taking at least 30 s to reach equilibrium in unbuffered solution, and considerably longer (~5 min) in the presence of intrinsic, intracellular buffers (Leem & Vaughan-Jones, 1998). Since reversible CO_2 hydration is catalysed by carbonic anhydrase (CA) and since CA activity is expressed (Bruns & Gros, 1992) and functionally active in cardiomyocytes (Lagadic-Gossmann *et al.* 1992; Leem & Vaughan-Jones, 1998), there may be an important role for

this enzyme in regulating intracellular H^+ ion mobility and hence the spatial distribution of intracellular pH. Evidence for the regulation of H_i^+ mobility by intracellular CA has emerged recently from confocal imaging of spatial pH_i non-uniformities induced by membrane acid transport in epithelial duodenal enterocytes (Stewart *et al.* 2000).

In the present work we have used the method of diffusing acid locally into a ventricular myocyte through a patch pipette in order to explore the effect of CO_2/HCO_3^- buffer and CA activity on the longitudinal movement of H_i^+ equivalents. Intracellular pH was monitored using AM-loaded SNARF, and apparent H_i^+ mobility was assessed by imaging intracellular pH (pH_i) using laser scanning confocal microscopy.

Preliminary reports of these experiments have been published previously (Vaughan-Jones *et al.* 2000*a*, *b*).

METHODS

Details are given in full in Methods of the accompanying paper (Vaughan-Jones *et al.* 2002). Briefly, ventricular myocytes were isolated enzymatically from hearts of New Zealand White rabbits (2–3 kg). The animals were anaesthetized with an intravenous injection of sodium pentobarbitone (50 mg kg^{-1}) and 0.5 ml heparin to prevent blood clotting, in accordance with national guidelines. Intracellular pH was measured ratiometrically in single cells during pipette acid loading using the fluorescent pH indicator SNARF-1 (loaded into the cell in its acetoxymethyl ester (AM) form) and a confocal microscope. Myocytes were held in the glass-bottomed cell chamber and continuously superfused at 36 ± 0.3 °C with a CO_2/HCO_3^--buffered solution containing (mM): NaCl 126.0, KCl 4.4, $MgCl_2$ 1.0, dextrose 11.0, $CaCl_2$ 1.1 and 18.5 Na HCO_3^-. It was continuously gassed with 5.0 % CO_2–95.0 % O_2 to give a pH of 7.4. The barometric pressure in the laboratory was ~640 mmHg, yielding a P_{CO_2} of ~30 mmHg. This solution also contained 1 mM amiloride (Sigma Chemical, St Louis, MO, USA) to inhibit Na^+–H^+ exchange. In some experiments 10 μM of the CA inhibitor acetazolamide (ATZ) (Sigma) was also included. This concentration of ATZ has been shown to inhibit maximally the influence of CA on the rate of intracellular CO_2 hydration in guinea-pig ventricular myocytes bathed in CO_2/HCO_3^--buffered solution (Leem & Vaughan-Jones, 1998). The composition of the pipette filling solution was the same as that described in the preceding paper (mM: KCl 140, dextrose 5.5, $MgCl_2$ 0.5, and HCl 1.0, pH = 3). It was gas equilibrated with 5.0 % CO_2–95.0 % O_2 immediately before use and held in a glass syringe at 37 °C before back-filling the pipettes.

Determination of intracellular buffer capacity

Total intracellular buffer capacity (β_{tot}) is equal to the sum of intrinsic buffer capacity (β_i) and CO_2-dependent buffer capacity (β_{CO_2}). As noted in the accompanying paper (Vaughan-Jones *et al.* 2002) we used the following empirical equation (Leem *et al.* 1999) to compute β_i:

$$\beta_i = \frac{2.3[A] \times 10^{(pH_i - pK_a)}}{(1 + 10^{(pH_i - pK_a)})^2} + \frac{2.3[B] \times 10^{(pH_i - pK_b)}}{(1 + 10^{(pH_i - pK_b)})^2}, \quad (1)$$

where A and B are two buffer populations of concentration 84.22 and 29.38 mM, respectively, and −log of dissociation constant (pK) values (pK_a and pK_b) of 6.03 and 7.57, respectively. β_{CO_2} was calculated as:

$$\beta_{CO_2} = 2.3[HCO_3^-]_i = 2.3[HCO_3^-]_o \times 10^{(pH_i - pH_o)}, \quad (2)$$

where $[HCO_3^-]_i$ and $[HCO_3^-]_o$ are the intra- and extracellular bicarbonate concentrations, respectively.

This assumes that the CO_2 solubility coefficient and the pK_a of CO_2/HCO_3^- are the same inside and outside the cell. It also assumes that the CO_2/HCO_3^- buffer system is at equilibrium.

Summarized results are presented as means ± S.E.M. Statistical analysis was performed using Student's t test for unpaired data. $P < 0.05$ was considered significant.

RESULTS

Effect of CO_2/HCO_3^- buffer on pH_i during intracellular acid loading by pipette

Acid loading in proximal and distal regions. Figure 1 compares the time course of acid loading in two confocal regions of interest (ROIs) defined within a myocyte superfused with either Hepes-buffered Tyrode solution (*A*) or CO_2/HCO_3^--buffered Tyrode solution (*B*), both at pH_o 7.4. In each case, an acid-filled (pH 3.0) patch pipette was attached to one end (the proximal end) of the cell. In the case of the CO_2/HCO_3^--buffered cell, care was taken to ensure that the pipette filling solution was also saturated with 5 % CO_2 at 37 °C. Ratiometric confocal images of pH_i were obtained at roughly 2 s intervals. Specimen ratiometric images are illustrated to the right of Fig. 1*A* and *B*. Throughout the present work, the centres of the two ROIs were standardized as close as possible to 16 μm (proximal ROI) and 58 μm (distal ROI) downstream from the pipette, as indicated in the images.

In Hepes buffer (Fig. 1*A*), the cell acidified following break-in with the pipette but, at the distal ROI, onset of acidification, measured at a threshold acidification of −0.1 ΔpH_i, was delayed by ~25 s (see Fig. 1*A*, inset) and proceeded more slowly, as reported in the accompanying paper (Vaughan-Jones *et al.* 2002). In contrast, in CO_2/HCO_3^- buffer (Fig. 1*B*), proximal and distal acidification rates were very similar and the distal delay for onset of acidification was reduced considerably to a few seconds (see Fig. 1*B*, inset).

Diffusion delay. To measure this, we used a protocol developed in the accompanying paper, where arrival of the diffusing acid within an ROI was measured at a threshold rise of 20 nM $[H^+]_i$ (this is, for example, equivalent to a 0.1 unit fall in pH_i from a starting pH_i of 7.10). The pH_i traces were therefore converted to changes in $[H^+]_i$ (for an illustration of this process see Fig. 8 of Vaughan-Jones *et al.* 2002). The procedure was adopted because inter-ROI time delay at a 20 nM threshold was used later for estimating D_{app}^H. The time delay was ~4-fold lower when using CO_2/HCO_3^--buffered superfusates. Mean delay in Hepes was 25.1 ± 5.1 s (n = 10; data from Fig. 6 of Vaughan-

Jones *et al.* 2002) whereas it was 5.93 ± 2.96 s (n = 7) in CO_2/HCO_3^-.

Longitudinal spatial profiles of pH_i. The reduced delay for intracellular H^+ equivalent movement in the presence of CO_2/HCO_3^- buffer implies that the longitudinal spatial profile for acid loading should be more uniform throughout the loading period. The accompanying paper (Vaughan-Jones *et al.* 2002) showed that, when using Hepes superfusates, a longitudinal pH_i gradient of 0.2–0.4 units was evident during acid loading. In the present work, when using CO_2/HCO_3^--buffered superfusates, no clear longitudinal gradient of pH_i could be resolved within ROIs drawn down the length of the cell (n = 7; not shown). A gradient, however, must have existed as distal acid loading lagged behind proximal loading by several seconds. The amplitude of longitudinal pH_i gradients under these conditions can be appreciated from the inset in Fig. 1*B* where linear fits to the proximal and distal acid loading traces suggest a spatial pH difference of 0.02–0.03 pH units. Resolving these small differences more clearly will require significant improvements in the signal-to-noise ratio of the pH_i traces. In conclusion, spatial uniformity of pH_i is enhanced greatly by CO_2/HCO_3^-, consistent with an increase in the mobility of intracellular acid equivalents.

Effect of acetazolamide on pH_i during acid loading by pipette

The experiment shown in Fig. 2 illustrates the effect of inhibiting CA with 10 μM of the membrane permeant CA inhibitor acetazolamide (ATZ). This agent has been shown to inhibit fully intracellular CA activity in ventricular

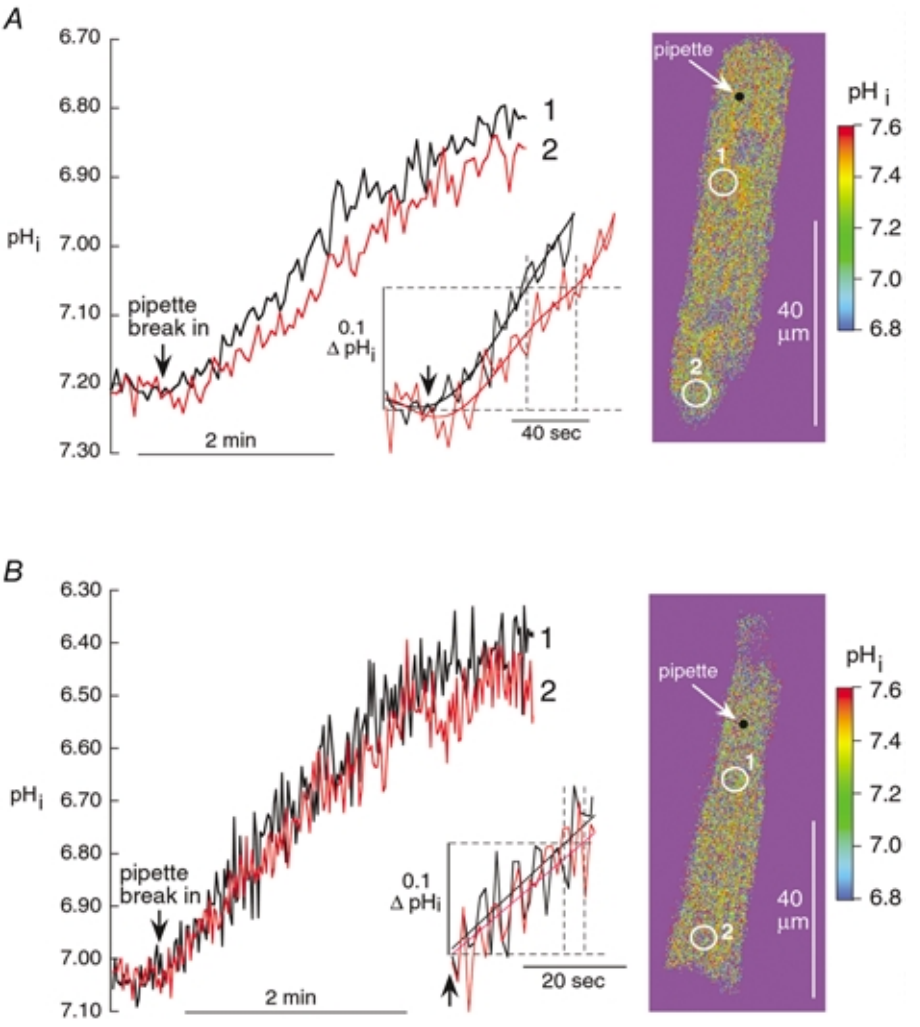

Figure 1. Longitudinal diffusion delay is reduced in CO_2/HCO_3^- buffer

Acid is diffused into a rabbit myocyte from a patch pipette. Standardized longitudinal positions of pipette and regions of interest (ROIs) are shown in a confocal, calibrated ratiometric SNARF image (right). Distance from pipette to centre of ROI 1: 15 μm; ROI 1 to ROI 2: 40 μm. Main graph shows the time course of acid loading averaged within the ROIs. Inset shows the initial period after break-in at higher amplification. To help identify the arrival time of pH_i at the 0.1 threshold, polynomial fits (5th order) were applied to each curve over the first 2.3 min. Dashed lines indicate time delay between the two ROIs estimated at a threshold fall of pH_i (ΔpH_i) of −0.1 units. *A*, Hepes-buffered superfusate. *B*, 5 % CO_2/HCO_3^--buffered superfusate.

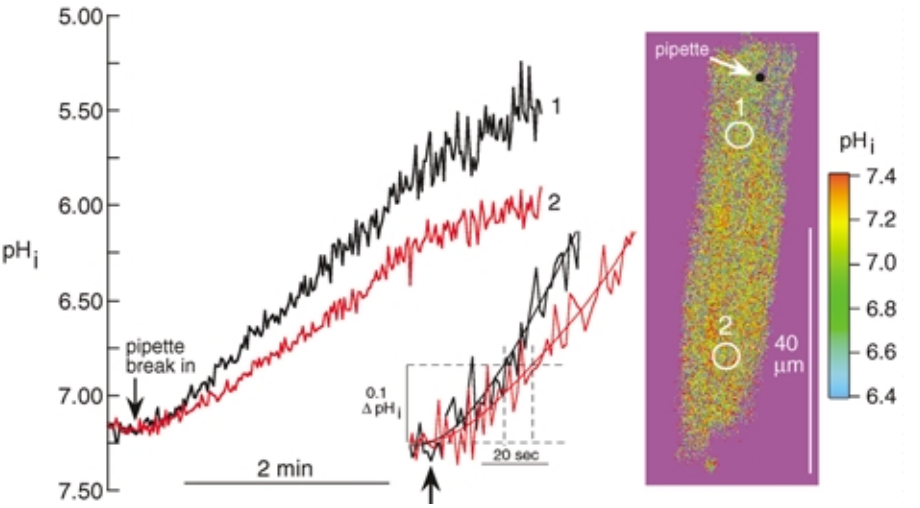

Figure 2. ATZ increases intracellular diffusion delay

Time course of acid loading averaged within ROIs 1 and 2 plotted in main graph. Calibrated ratiometric image shows standardized longitudinal positions of pipette and the two ROIs (see legend to Fig. 1 for quantitative spacing). Inset shows the initial period after break-in at higher amplification. Continuous lines fitted to traces by computer (8th order polynomial). Dashed lines indicate diffusion delay (at a −0.1 ΔpH_i threshold level).

cardiomyocytes (Leem & Vaughan-Jones, 1998). Despite the fact that CO_2/HCO_3^- buffer was present, the distal ROI acidified more slowly than the proximal ROI and, as shown in the inset, there was a delay of several seconds between the proximal and distal regions. In eight cells superfused with CO_2/HCO_3^-, the average inter-ROI time delay in the presence of ATZ (measured at a threshold rise of 20 nM $[H^+]_i$) was 15.53 ± 2.65 s (n = 8), 2.6 times longer than in the absence of the drug. The result indicates that while CO_2/HCO_3^- buffer can facilitate intracellular H^+ equivalent movement, efficient facilitation requires the activity of intracellular CA.

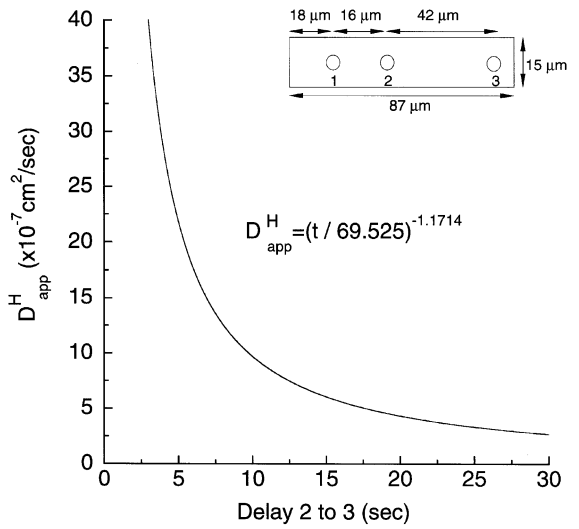

Figure 3. Relationship between inter-ROI time delay and apparent H_i^+ mobility

Results of the mathematical model of H_i^+ diffusion described in previous paper (Vaughan-Jones *et al.* 2002). Graph drawn according to the equation: D^H_{app} = (delay/69.525)$^{-1.1714}$. Delay was measured in a model cell (at a 20 nm threshold rise of $[H^+]_i$) between points 2 and 3 downstream from a pipette sited at point 1 (see inset for dimensions and point positions of model cell). The relationship is shown for time delays of 2–14 s. The equation was derived empirically from time courses predicted by the model for the rise of acid at sites 2 and 3 (for further details see Fig. 11 of Vaughan-Jones *et al.* 2002).

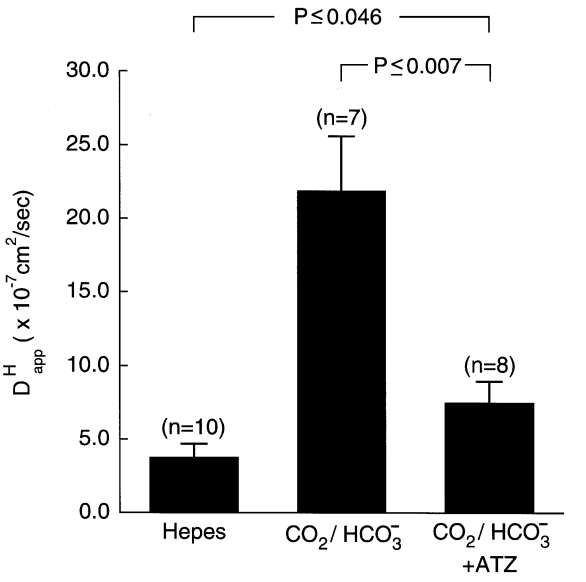

Figure 4. H_i^+ mobility coefficient is increased by 5 % CO_2/HCO_3^- but this increase is attenuated by ATZ

The number of cells is shown in parentheses. ATZ dose = 10 μM. The results of Student's unpaired t test are indicated above the bars.

Apparent H_i^+ diffusion coefficient in CO_2/HCO_3^-

In the accompanying paper (Vaughan-Jones *et al.* 2002) we showed that, for a given longitudinal separation of ROIs downstream from the pipette, the time delay for acid movement between the ROIs provided a useful assessment of D_{app}^H (see Fig. 10*B* of Vaughan-Jones *et al.* 2002). In that paper, a mathematical model was developed to describe the spatiotemporal properties of $[H^+]_i$ accumulation in response to continuous diffusion of H^+ from the pipette. It was shown that, for a specified set of cell parameters (given at the top of Fig. 3 of the present paper), inter-ROI time delay (t) could be described empirically as:

$$t = 69.525\,(D_{app}^H)^{-0.8537},$$

which, on rearrangement gives:

$$D_{app}^H = (t/69.525)^{-1.1714}, \quad (3)$$

where time for first appearance of diffusing acid within an ROI was taken at a threshold rise ($\Delta[H^+]_i$) of 20 nM. Equation (3) gave a good fit to experimental data derived in the absence of CO_2/HCO_3^- (Vaughan-Jones *et al.* 2002). The function is essentially hyperbolic, and has been plotted as the continuous line in Fig. 3. For convenience, we have used this function to estimate D_{app}^H from measurements of time delay in the present experiments, while matching our experimental cell parameters as closely as possible to those specified in the mathematical model (see Fig. 3 legend for details).

Values for D_{app}^H, obtained by substituting time delay into eqn (3), were averaged and have been plotted in the histogram shown in Fig. 4. Also plotted is the mean value for D_{app}^H estimated previously in Hepes (taken from Vaughan-Jones *et al.* 2002). The D_{app}^H estimated in CO_2/HCO_3^--buffered conditions was 21.89×10^{-7} cm^2 s^{-1}, which is nearly 6-fold higher than that determined in Hepes. This higher value is reduced in the presence of ATZ to 7.53×10^{-7} cm^2 s^{-1}, a value approaching that estimated in Hepes.

DISCUSSION

Intracellular CO_2/HCO_3^- facilitates H_i^+ ion movement

Facilitation is regulated by carbonic anhydrase. The effective H_i^+ diffusion coefficient in the mammalian ventricular myocyte is enhanced nearly 6-fold in the presence of a CO_2/HCO_3^- buffer system. In the absence of CO_2/HCO_3^-, net diffusive flux of intrinsic buffer will be greater than H^+ flux (because intrinsic, mobile buffer concentration $\gg [H^+]_i$) and will therefore govern overall H^+ ion movement (Vaughan-Jones *et al.* 2002). Adding sufficient concentration of a more mobile, extrinsic buffer, such as CO_2/HCO_3^-, will short circuit the intrinsic buffer shuttle by adding a faster shuttle, resulting in a faster apparent mobility of H_i^+.

Previous models of intracellular proton mobility (Junge & McLaughlin, 1987; Irving *et al.* 1990) did not consider the potential importance of CO_2/HCO_3^- buffer (carbonic buffer). The present work shows that the increase in D_{app}^H upon addition of carbonic buffer dramatically reduces the spatial non-uniformity of pH_i caused by local acid influx. In addition, inhibiting intracellular CA activity removes most of this effect. This is similar to a recent report by Stewart *et al.*, (2000) where addition of ATZ to an isolated duodenal enterocyte removed the ability of carbonic buffer to attenuate spatial pH_i gradients elicited by membrane H^+ transport. This suggests that regulation of H_i^+ mobility by CA may be a fundamental role of the enzyme.

Regulation of H^+ mobility by CA need not be restricted to the intracellular compartment. Extracellular CA isoforms that are membrane bound (Dodgson, 1991) are expressed not only in heart (De Hemptinne *et al.* 1987) but also in various other tissues (Geers & Gros, 2000; Tong *et al.* 2000*a*). These extracellular sites may therefore help to reduce the possibility of local pH_o non-uniformity. Such a role would be particularly important in unstirred interstitial spaces such as those within the CNS where significant local changes of pH_o are known to occur (Sykova *et al.* 1988; Tong e*t al.* 2000*b*; Menna *et al.* 2000).

Cardiac carbonic anhydrase. Functional expression of CA_i in heart is modest (Bruns & Gros, 1992), in that it catalyses the hydration rate of intracellular CO_2 ~3-fold (Leem & Vaughan-Jones, 1998) as compared with erythrocytes where catalysis is ~17000-fold (Forster, 1969). The low catalytic levels in heart may represent an ideal level of CA_i function: sufficient to enhance intracellular D_{app}^H and hence reduce spatiotemporal non-uniformity of pH_i, but low enough to allow most metabolically produced CO_2 to escape from the cell.

All cardiac CA appears to be bound to SR and sarcolemmal membranes (Bruns & Gros, 1992) (cytosolic isoforms have not so far been identified). A membrane-bound CA may suffice to catalyse intracellular H^+ ion mobility provided some of its active sites are cytoplasmically oriented. The SR in ventricular myocytes interdigitates with t-system membranes, so that most areas of cytoplasm should be within a few micrometres of a catalytic site. Even in cardiac cells that lack a t-system, such as atrial and Purkinje cells, the SR remains highly branched in the transverse direction (Cordeiro *et al.* 2001) so that CA active sites should still be available throughout the cytoplasmic compartment. An SR- and sarcolemmal-bound CA could therefore readily function as the regulatory site for carbonic facilitation of H^+ mobility in the cardiomyocyte.

How does CA regulate H_i^+ mobility?

H^+ ions entering the cell from a patch pipette are buffered proximally by intracellular HCO_3^- forming carbonic acid that dissociates into CO_2 and water (illustrated in Fig. 5).

Table 1. Apparent diffusion coefficients ($cm^2\ s^{-1}$) derived for intracellular, mobile intrinsic and extrinsic (CO_2/HCO_3^-) buffer

Intrinsic	Extrinsic	
D_{mob}	D_{carb} (with CA)	D_{carb} (no CA)
8.9×10^{-7}	44.7×10^{-7}	12.2×10^{-7}

While some CO_2 diffuses out of the cell across the sarcolemma, some diffuses longitudinally to more distal (more alkaline) intracellular regions. There it is rehydrated, thus regenerating H^+ and HCO_3^- ions. Some downstream diffusion of carbonic acid may also occur in parallel with CO_2, again producing HCO_3^- distally. By these mechanisms H^+ ions have, in effect, moved from a proximal to a distal region of the cell, although the H^+ ions appearing distally are not the same as those injected proximally. The HCO_3^- that is regenerated distally then diffuses back towards proximal regions where it is available to buffer more acid diffusing from the pipette. On the scheme shown in Fig. 5, intracellular acid moves on a CO_2/HCO_3^- shuttle, downstream via CO_2 (or H_2CO_3) and upstream via HCO_3^- diffusion.

The shuttle is catalysed at two points by CA. These are the two chemical steps where CO_2 and HCO_3^- are reversibly interconverted. The fact that carbonic buffer greatly increases apparent H_i^+ mobility would be consistent with turnover rate of this shuttle being faster than that of intrinsic mobile buffers (for a description of the intrinsic shuttle see Fig. 11 (top panel) of Vaughan-Jones *et al.* 2002). Thus the 'effective mobility' of carbonic buffer appears faster than that of intrinsic buffers.

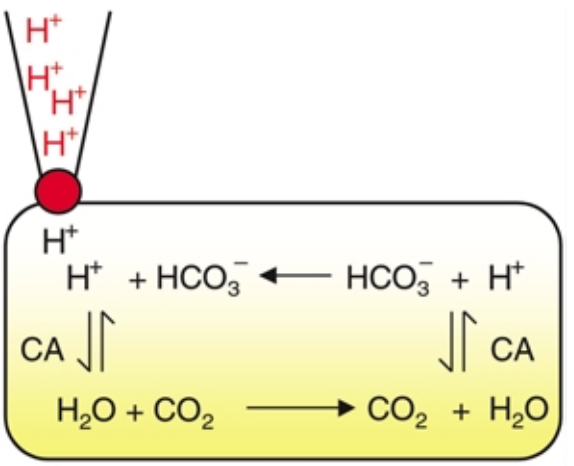

Figure 5

Intracellular carbonic buffer shuttle showing longitudinal diffusion of CO_2 and HCO_3^- and carbonic anhydrase (CA)-catalysed reversible hydration of CO_2.

Evidence for the above model comes from the effect of inhibiting CA with ATZ. This slows the two chemical steps and, if one of these were to become rate limiting, the turnover of the shuttle would slow thus decreasing D_{app}^H, as indeed found experimentally (Fig. 2). In the absence of CA activity, the rate constant for CO_2 hydration is known to be slow (0.144 s^{-1}, ~400-fold slower than the reverse step (e.g. Swenson & Maren, 1978; Leem & Vaughan-Jones, 1998) and is likely to be the rate-limiting step. Furthermore, the observation that ATZ reduces D_{app}^H to a value more similar to that seen in the absence of carbonic buffer (Fig. 4) suggests that turnover of the carbonic shuttle is now comparable to that of the intrinsic shuttle.

Effective mobility of CO_2 and non-CO_2 buffers in the ventricular myocyte

Provided intracellular buffers are not saturated, the apparent H_i^+ diffusion coefficient (D_{app}^H) can be approximated as the sum of several terms defining the mobility and fractional buffer capacity of each of the component buffers (Junge & McLaughlin, 1987; Irving *et al.* 1990):

$$D_{app}^H = (2.3[H^+]_i D_H)/\beta_{tot} + \sum\{(\beta D_\beta)/\beta_{tot}\}, \quad (4)$$

where D_H is the diffusion coefficient for H^+ ions in dilute, unbuffered solution (0.9×10^{-4} $cm^2\ s^{-1}$ at 25 °C; Vanysek, 1999), β is the buffer capacity for a given type of intracellular buffer of diffusion coefficient D_β, and β_{tot} is the total intracellular buffer capacity (equal to the sum of all intrinsic and CO_2-dependent buffer capacities).

At physiological pH_i, the first term on the right side of eqn (4) $\ll$ the other terms, and can be ignored. For a cell bathed in CO_2/HCO_3^--buffered Tyrode solution, the right hand terms will include intrinsic and carbonic buffers.

$$D_{app}^H = (D_{mob}\beta_{mob})/\beta_{tot} + (D_{carb}\beta_{CO_2})/\beta_{tot}, \quad (5)$$

where D_{mob} and β_{mob} are, respectively, the diffusion coefficient lumped for all mobile intrinsic buffers (8.9×10^{-7} $cm^2\ s^{-1}$) and their summed buffer capacity (11.4 mM/pH unit; Vaughan-Jones *et al.* 2002). D_{carb} and β_{CO_2} are, respectively, the effective diffusion coefficient and buffer capacity (eqn (2)) of intracellular carbonic buffer. Note that D_{carb} does not represent the diffusion coefficient of a specified solute. It is a theoretical term, governed by the rate constants of the carbonic shuttle shown in Fig. 5. By comparing D_{carb} with the diffusion coefficient for intrinsic buffer (D_{mob}), one may assess the effectiveness of the two buffer systems at mediating spatial H^+ movement. Equation (5) has been used to estimate D_{carb} using the mean values of D_{app}^H in Hepes and in CO_2/HCO_3^- ± ATZ (data from Fig. 4). These estimates are shown in Table 1, along with the value of D_{mob}. The effective mobility for carbonic buffer, D_{carb} (4.47×10^{-6} $cm^2\ s^{-1}$), is 5-fold higher than for D_{mob}. Interestingly, D_{carb} is reduced ~4-fold in the presence of ATZ, consistent with the suggestion (previous

section) that intrinsic and carbonic buffer mobility are comparable once CA activity is inhibited.

Comparison of facilitated H_i^+ diffusion with facilitated diffusion of CO_2

There is evidence that carbonic buffer can also facilitate the diffusion of CO_2 within unstirred compartments For example, up to half of the CO_2 flux across the extracellular unstirred layer (100 μm thick) of a skeletal muscle fibre is believed to occur via a facilitated mechanism (Geers & Gros, 2000). This facilitation occurs through hydration of CO_2 to HCO_3^- which then diffuses across the unstirred layer whereupon it is reconverted to CO_2, the CO_2 transformations being catalysed by CA. There are therefore strong similarities between the facilitation of spatial H^+ and CO_2 movements, both relying upon the diffusion of HCO_3^- and the activity of CA. There are, however, important differences: facilitated H^+ diffusion requires the back diffusion of HCO_3^- in a shuttle mechanism (see Fig. 5), while facilitated CO_2 diffusion requires a forward movement of protonated intrinsic buffers in parallel with the HCO_3^- diffusion (for a review of facilitated CO_2 diffusion see Geers & Gros, 2000).

Do spatiotemporal gradients of pH_i occur physiologically in the heart?

Longitudinal gradients persist in CO_2/HCO_3^-. Following a local influx of acid (e.g. from a pipette or via a pH transporter), spatiotemporal gradients of intracellular H^+ equivalents must occur, the question is whether they are large enough and sufficiently sustained to be of physiological significance. Figure 6 shows theoretical reconstructions of the longitudinal H_i^+ gradients induced by diffusion from an acid-filled pipette. These were obtained from the mathematical model described in the accompanying paper (Vaughan-Jones *et al.* 2002) while using typical values for D_{app}^H in the absence (Fig. 6*A*) and presence (Fig. 6*B*) of carbonic buffer.

In the absence of carbonic buffer (Fig. 6*A*), a considerable pH_i gradient is predicted during acid loading. For example, 35 s after break-in, a $\Delta[H^+]_i$ of 107 nM extends from the pipette to the distal end of the cell. This is equivalent to a longitudinal ΔpH_i of 0.32 units (assuming initial pH_i was 7.1), a gradient comparable to that seen experimentally (for example see Fig. 7 of Vaughan-Jones *et al.* 2002). In the presence of carbonic buffer (Fig. 6*B*), a longitudinal pH_i gradient is still predicted, but its amplitude is considerably reduced to about 20 nM, equivalent to 0.06 ΔpH_i units at 35 s, and 0.04 at 80 s, again comparable to that estimated experimentally.

The above simulations illustrate that pH_i microdomains persist for several tens of seconds in the presence of CO_2/HCO_3^-, but their peak amplitude is typically < 0.1 pH units. Although modest, if such spatial differences of pH_i occurred naturally, they would exert significant effects within a myocyte, given the high pH sensitivity of many spatially distributed intracellular proteins such as myofilaments (Fabiato & Fabiato, 1978), sarcolemmal channels (Irisawa & Sato, 1986) and transporters (Philipson *et al.* 1982), and SR Ca^{2+} release channels (Meissner & Henderson, 1987; Choi *et al.* 2000; Balnave & Vaughan-Jones, 2000).

Radial gradients. Acid diffusion from the pipette was ~10 mM l^{-1} min^{-1}, comparable to whole-cell acid efflux on sarcolemmal Na^+–H^+ exchange at pH_i 6.5 (Leem *et al.*

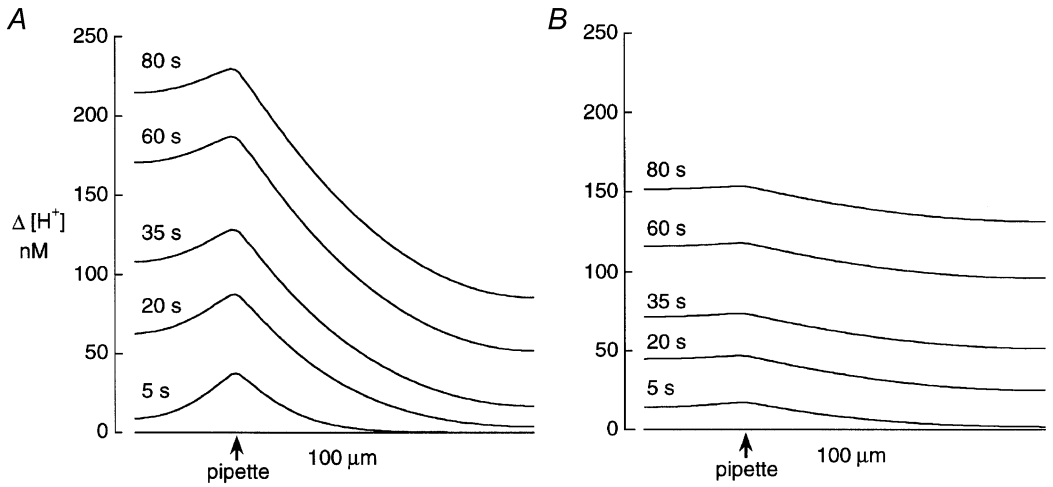

Figure 6. Modelling the longitudinal profile of $[H^+]_i$ during acid diffusion from a patch pipette

The model shows profiles predicted at different times after break-in, displayed as $\Delta[H^+]_i$ (nM), the increase above control levels. Length of model cell, 100 μm; width, 15 μm. Diameter pipette tip, 2 μm. Pipette site, 25 μm from left end of model cell and positioned 7.5 μm from the longitudinal edge. *A*, CO_2/HCO_3^--free conditions with $D_{app}^H = 3.8 \times 10^{-7}$ cm^2 s^{-1}. *B*, CO_2/HCO_3^--buffered conditions with $D_{app}^H = 22.0 \times 10^{-7}$ cm^2 s^{-1}. Model taken from Vaughan-Jones *et al.* (2002).

1999), thus raising the possibility of physiologically relevant pH_i gradients being generated radially during pH_i regulation (Vaughan-Jones *et al.* 2002). Carbonic buffer will attenuate these pH_i gradients, especially in myocytes with invaginated t-system membranes which express pH transporters. In cells lacking a t-system, however (e.g. atrial and Purkinje cells), modelling suggests that radial gradients may still occur in some cardiac cells in CO_2/HCO_3^--buffered conditions (say, $\leqslant 0.05$ pH units), given that surface to core (i.e. radial) distances in Purkinje myocytes can be ~15 μm in rabbit (Cordeiro *et al.* 1998) and up to 30 μm in dog (Boyden *et al.* 1989). One aim of future experimental work must be to assess the existence of radial pH microdomains.

H_i^+ facilitation should disappear at low pH_i; relevance to myocardial ischaemia?

One assumption in the simulations illustrated in Fig. 6 is that D_{app}^H remains constant during acid loading. While the simulations reproduce many features observed experimentally, we do not exclude the possibility that effective H^+ mobility may vary, particularly during large changes of pH_i. As pointed out previously (Al Baldawi *et al.* 1992; Vaughan-Jones *et al.* 2002) D_{app}^H may decrease as mobile intrinsic buffers with p*K* values in the physiological range become saturated at low pH_i. Facilitation of H_i^+ mobility by carbonic buffer may also fail at low pH_i, especially during episodes of metabolic acidosis. Under these conditions intracellular HCO_3^- concentration decreases and, at a sufficiently low bicarbonate level, turnover of the carbonic shuttle will effectively cease (given that β_{CO_2} in the second term on the right side of eqn (5) is proportional to $[HCO_3^-]_i$). The important role of CO_2/HCO_3^- in regulating spatial pH_i uniformity will therefore be compromised during metabolic acid overload. This also predicts that facilitation by carbonic buffer may be compromised during pathological disorders, such as myocardial ischaemia, that are associated with severe metabolic acidosis. Intracellular pH non-uniformity may therefore be more prevalent under these conditions.

Conclusions

Given the ubiquitous nature of the CO_2/HCO_3^- buffer in eukaryotic cells, its facilitation of H_i^+ mobility is likely to be a fundamental role. The fact that facilitation requires intracellular CA activity, an enzyme also commonly expressed in eukaryotic cells, suggests that regulation of spatio-temporal pH uniformity is a major function of the enzyme.

REFERENCES

Al-Baldawi, N. F. & Abercrombie, R. F. (1992). Cytoplasmic hydrogen ion diffusion coefficient. *Biophysical Journal* **61**, 1470–1479.

Balnave, C. D. & Vaughan-Jones, R. D. (2000). Effect of intracellular pH on spontaneous Ca^{2+} sparks in rat ventricular myocytes. *Journal of Physiology* **528**, 25–37.

Boyden, P. A., Albala, A. & Dresdner, K. P. (1989). Electrophysiology and ultrastructure of canine subendocardial Purkinje cells isolated from control and 24-hour infarcted hearts. *Circulation Research* **65**, 955–970.

Bruns, W. & Gros, G. (1992). Membrane-bound carbonic anhydrase in the heart. *American Journal of Physiology* **262**, H577–584.

Choi, H. S., Trafford, A. W., Orchard, C. H. & Eisner, D. A. (2000). The effect of acidosis on systolic Ca^{2+} and sarcoplasmic reticulum calcium content in isolated rat ventricular myocytes. *Journal of Physiology* **529**, 661–668.

Cordeiro, J. M., Spitzer, K. W. & Giles, W. R. (1998). Repolarizing K^+ currents in rabbit heart Purkinje cells. *Journal of Physiology* **508**, 811–823.

Cordeiro, J. M., Spitzer, K. W., Giles, W. R., Ershler, P. E., Cannell, M. B. & Bridge, J. H. B. (2001). Location of the initiation site of calcium transients and sparks in rabbit heart Purkinje cells. *Journal of Physiology* **531**, 301–314.

De Hemptinne, A., Marrannes, R. & Vanheel, B. (1987). Surface pH and the control of intracellular pH in cardiac and skeletal muscle. *Canadian Journal of Physiology and Pharmacology* **65**, 970–977.

Dodgson, S. J. (1991). The carbonic anhydrase. In *The Carbonic Anhydrases: Cellular Physiology and Molecular Genetics*, ed. Dodgson, S. J., Tashian, R. E., Gros, G. & Carter, N. D., pp. 3–14. Plenum Press, London.

Fabiato, A. & Fabiato, F. (1978). Effects of pH on the myofilaments and the sarcoplasmic reticulum of skinned cells from cardiac and skeletal muscles. *Journal of Physiology* **276**, 233–255.

Forster, R. E. (1969). The rate of CO_2 equilibrium between red cells and plasma. In *CO_2: Chemical, Biological, and Physiological Aspects*, ed. Forster, R. E., Edsall, J. T., Otis, A. B. & Roughton, F. J. W., pp. 275–286. NASA SP-188, Washington.

Geers, C. & Gros, G. (2000). Carbon dioxide and carbonic anhydrase in blood and muscle. *Physiological Reviews* **80**, 681–715.

Irisawa, H. & Sato, R. (1986). Intra- and extracellular actions of protons on the calcium current of isolated guinea pig ventricular cells. *Circulation Research* **59**, 348–355.

Irving, M., Maylie, J., Sizto, N. L. & Chandler, W. K. (1990). Intracellular diffusion in the presence of mobile buffers. Application to proton movement in muscle. *Biophysical Journal* **57**, 717–721.

Junge, W. & McLaughlin, S. (1987) The role of fixed and mobile buffers in the kinetics of proton movement. *Biochimica et Biophysica Acta* **890**, 1–5.

Kushmerick, M. J. & Podolsky, R. J. (1969). Ionic mobility in muscle cells. *Science* **166**, 1297–1298.

Lagadic-Gossmann, D., Buckler, K. J. & Vaughan-Jones, R. D. (1992). Role of bicarbonate in pH recovery from intracellular acidosis in the guinea-pig ventricular myocyte. *Journal of Physiology* **458**, 361–384.

Leem, C. H., Lagadic-Gossmann, D. & Vaughan-Jones, R. D. (1999). Characterization of intracellular pH regulation in the guinea-pig ventricular myocyte. *Journal of Physiology* **517**, 159–180.

Leem, C. H. & Vaughan-Jones, R. D. (1998). Out-of-equilibrium pH transients in the guinea-pig ventricular myocyte. *Journal of Physiology* **509**, 471–485.

Meissner, G. & Henderson, J. S. (1987). Rapid calcium release from cardiac sarcoplasmic reticulum vesicles is dependent on Ca^{2+} and is modulated by Mg^{2+}, adenosine nucleotide, and calmodulin. *Journal of Biological Chemistry* **262**, 3065–3073.

Menna, G., Tong, C. K. & Chesler, M. (2000). Extracellular pH changes and accompanying cation shifts during ouabain-induced spreading depression. *Journal of Neurophysiology* **83**, 1338–1345.

PHILIPSON, K. D., BERSOHN, M. M. & NISHIMOTO, A. Y. (1982). Effects of pH on Na^+-Ca^{2+} exchange in canine cardiac sarcolemmal vesicles. *Circulation Research* **50**, 287–293.

STEWART, A. K., BOYD, C. A. R. & VAUGHAN-JONES, R. D. (2000). A novel role for carbonic anhydrase: pH gradient dissipation in mouse small intestinal enterocytes. *Journal of Physiology* **516**, 209–217.

SWENSON, E. R. & MAREN, T. H. (1978). A quantitative analysis of CO_2 transport at rest and during maximal exercise. *Respiratory Physiology* **35**, 129–159.

SYKOVA, E., SVOBODA, J., CHVATAL, A. & JENDELOVA, P. (1988). Extracellular pH and stimulated neurons. *Ciba Foundation Symposium* **139**, 220–235.

TONG, C. K., BRION, L. P., SUAREZ, C. & CHESLER, M. (2000*a*). Interstitial carbonic anhydrase (CA) activity in brain is attributable to membrane-bound CA type IV. *Journal of Neuroscience* **20**, 8247–8253.

TONG, C. K., CAMMER, W. & CHESLER, M. (2000*b*). Activity-dependent pH shifts in hippocampal slices from normal and carbonic anhydrase II-deficient mice. *Glia* **31**, 125–130.

VANYSEK, P. (1999). Ionic conductivity and diffusion at infinite dilution. In *CRC Handbook of Chemistry and Physics*, section 5, *Thermochemistry, Electrochemistry and Kinetics*, ed. LIDE, D. R., 79th edn, pp. 93–95. CRC Press, London.

VAUGHAN-JONES, R. D., ERSHLER, P. R., SKOLNICK, R. L. & SPITZER, K. W. (2000*a*). Slow intracellular H^+ mobility regulated by carbonic anhydrase activity in rabbit ventricular myocytes. *Biophysical Journal* **78**, 223A.

VAUGHAN-JONES, R. D., ERSCHLER, P., SKOLNICK, R. & SPITZER, K. W. (2000*b*). Intracellular H^+ mobility is facilitated by carbonic anhydrase activity in rabbit ventricular myocytes. *Journal of Physiology* **527.P**, 67*P*.

VAUGHAN-JONES, R. D., PEERCY, B. E., KEENER, J. P. & SPITZER, K. W. (2002). Intrinsic H^+ ion mobility in the rabbit ventricular myocyte. *Journal of Physiology* **541**, 139–158.

Acknowledgements

This study was supported by grants from the National Heart, Lung, and Blood Institute (HL-42873) and the Nora Eccles Treadwell Foundation to K.W.S. and by grants from the British Heart Foundation and the Wellcome Trust to R.D.V.-J. We thank Dr P. R. Ershler for assistance with the confocal imaging.